Available online at www.sciencedirect.com
ScienceDirect
Journal of Power Sources 162 (2006) 765–772
JOURNAL OF POWER SOURCES
www.elsevier.com/locate/jpowsour

The direct borohydride fuel cell for UUV propulsion power

J. Barry Lakeman [a], Abigail Rose [a,*], Kevin D. Pointon [a], Darren J. Browning [a], Keith V. Lovell [b], Susan C. Waring [b], Jackie A. Horsfall [b]

[a] *Physical Sciences, Dstl Porton Down, Salisbury SP4 0QR, UK*
[b] *Department of Materials & Medical Sciences, Cranfield University, Shrivenham Campus, Swindon SN6 8LA, UK*

Received 8 February 2005
Available online 18 August 2005

Abstract

The development of proton exchange membrane and direct methanol fuel cell stacks is now well advanced for many applications. However, the significant performance advantages that these have over the battery for small to moderate scale applications will not be realised until a credible fuel source has been developed. The deficiencies of the PEMFC and DMFC can be eliminated by cation or anion-conducting membranes incorporated into a direct sodium borohydride fuel cell (DSBFC). The characterisation of membranes for the DSBFC is discussed. Novel membranes have been prepared which have resistance of an equal magnitude to the commercially available Nafion® membrane.

Keywords: Direct sodium borohydride fuel cell; Unmanned underwater vehicles; Propulsion

1. Introduction

Owing to the size constraints of unmanned underwater vehicles (UUV's), the energy density of the power source needs to be fully optimised. Currently, most UUVs are powered by silver–zinc, lead–acid or lithium ion batteries. However, the energy density of these technologies is limited, resulting in short endurance times. The use of a high energy density power source such as a fuel cell could increase endurance times or reduce the overall platform weight. Table 1 shows comparison data for current and future power sources.

The figures in Table 1 show that the energy density of fuel cell technology is almost an order of magnitude greater than that of current batteries. Therefore, fuel cells have the potential to overcome the limitations of batteries for UUV applications.

The direct methanol and PEM fuel cell are amongst the most technologically advanced low temperature fuel cell technologies owing to the extensive funds provided for their development in the communications and automotive industries. However, the construction of a direct methanol fuel cell (DMFC) using the proton-exchange membrane (PEM) has severe performance limitations when compared to its hydrogen fuelled PEMFC equivalent, owing to the sluggish methanol oxidation kinetics and the mass transport limitations of the methanol. In addition, the DMFC is hampered by methanol crossover through the electrolyte membrane, caused by diffusion and electro-osmotic drag (see Fig. 1). This results in a mixed cathode potential and a reduction in power output. The DMFC is also unattractive because of the toxicity of methanol and the production of carbon dioxide, which leads to problems of carbon dioxide rejection and fuel loss.

The DSBFC has many advantages over other direct liquid fuel cells, of which the DMFC is the most developed. The kinetics of borohydride oxidation appear far more facile than those of methanol oxidation, making the power density of the DSBFC potentially superior to that of the DMFC. This makes it more suitable for portable applications, operating at ambient temperatures, and also allows for easy cell start up. In addition, the DSBFC does not appear to suffer from the depolarising effect of fuel crossover to the same

* Corresponding author. Tel.: +44 1980 614943; fax: +44 1980 613611.
E-mail address: arose@dstl.gov.uk (A. Rose).

0378-7753/$ – see front matter.
doi:10.1016/j.jpowsour.2005.07.022

Table 1
Energy density of UUV power source technology

Power source	Gravimetric energy density ($Wh\,kg^{-1}$)	Volumetric energy density ($Wh\,l^{-1}$)	Notes
Silver–zinc battery[a]	81	174	Good energy density but expensive, often used for specialist applications. Limited cycles
Lead–acid battery[b]	35	53	Low energy density but proven technology
Lithium ion battery[c]	128	315	Currently the most advanced rechargeable battery type
Direct borohydride fuel cell (solid fuel)	950 (operating at 50% efficiency)	2850	Technology still in the development phase. Fuel and products easy to handle. Increasing stealth over the DMFC
Direct methanol fuel cell (neat methanol)	690 (operating at 30% efficiency)	2070	A more developed technology than the DSBFC with good energy density, but the gaseous product would reduce stealth if released or would need additional hardware to dissolve gas before release.
PEMFC (H_2 fuelled)	690 (operating at 50% efficiency)	2070	Technology well developed, but would need a hydrogen source, reducing the volumetric energy density due to low hydrogen storage capacity

These values assume cells operating at their nominal voltage. The oxidant is assumed to be liquid oxygen. Hydrogen assumed to be stored in a 4 wt% hydrogen storage cylinder. Values based on 2 kW average power for 20 h.
[a] Saft rechargeable silver–zinc batteries, www.saftbatteries.com.
[b] Yuasa valve regulated lead acid rechargeable batteries, www.allbatteries.com.
[c] Saft Li-ion cells, www.saftbatteries.com.

degree as the DMFC, which requires dilution of the methanol fuel in order to reduce the crossover rate to an acceptable level. The DSBFC can, in theory, use non-platinum catalysts, and unlike methanol, sodium borohydride is non-flammable, relatively non-toxic, unless ingested and does not produce gaseous products, such as the carbon dioxide produced in the DMFC.

The reduction in tendency to fuel crossover in the alkaline fuel cell is illustrated in Fig. 1 by considering the alkaline and acid DMFCs, the former using a hydroxyl ion-conducting membrane, the latter an acid proton-conducting membrane. In the alkaline DMFC, the electro-osmotic drag opposes the tendency for fuel crossover, whereas in the acid DMFC the electro-osmotic drag exacerbates fuel crossover.

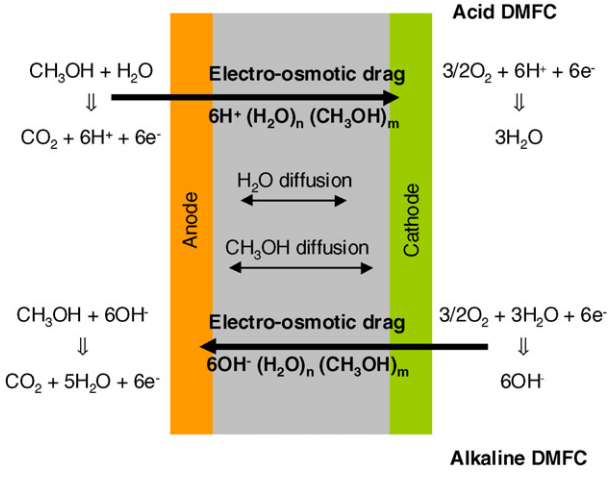

Fig. 1. Schematic representation of the reaction schemes for the traditional acid DMFC and its alkaline counterpart, illustrating how the electro-osmotic drag in the alkaline version counteracts fuel crossover.

The DSBFC can also be operated in two ways, with either an anion exchange membrane (AEM) or cation exchange membrane (CEM). The situation in the AEM-DSBFC is similar to the alkaline DMFC. At the onset of fuel oxidation, hydroxyl ions move from cathode to anode, counteracting the natural diffusion of the borohydride fuel. Consequently, it is anticipated that higher fuel concentrations can be tolerated in the anolyte of the DSBFC than in the traditional acid DMFC. When run with the CEM the charge balance is maintained by the movement of sodium ions from the anode to cathode. However, this route has some additional problems in that it would require recirculation of sodium ions to the anode for long-term use.

The reactions occurring in the DSBFC when oxygen is the oxidant are given by [1]:

$$\text{Anode}: \quad BH_4^- + 8OH^- \rightarrow BO_2^- + 6H_2O + 8e^- \quad E^0 = -1.24\,V \tag{1}$$

$$\text{Cathode}: \quad 2O_2 + 4H_2O + 8e^- \rightarrow 8OH^- \quad E^0 = 0.40\,V \tag{2}$$

$$\text{Overallreaction}: \quad BH_4^- + 2O_2 \rightarrow BO_2^- + 2H_2O \quad E^0{}_{Cell} = 1.64\,V \tag{3}$$

The oxidation of $NaBH_4$ liberates eight electrons and, therefore, the capacity of the pure compound is 5667 $Ah\,kg^{-1}$.

Multiplying by the cell voltage gives a theoretical energy density of 9293 $Wh\,kg^{-1}$. However, the solid sodium borohydride must be dissolved in aqueous solution, typically 20–50 wt%, which proportionally reduces the maximum

Table 2
Sodium borohydride vs. methanol as a direct fuel

	Sodium borohydride	Methanol
Cell reaction free energy change ($kJ\,mol^{-1}$)	−1273	−703
Theoretical specific energy ($Wh\,kg^{-1}$)	9300	6100
Theoretical specific charge capacity ($Ah\,kg^{-1}$)	5600	5000
Gibbs voltage (V)	1.64	1.21

achievable energy density. Table 2 below summarises the theoretical differences between the direct sodium borohydride cell and the direct methanol fuel cell.

A key factor in the successful development of the DSBFC is realising the full potential of the energy stored within the fuel solution. To a degree, this is compromised by the following hydrolysis reaction, which reduces the fuel utilisation:

$$BH_4^- + 2H_2O \rightarrow BO_2^- + 4H_2 \quad (4)$$

Reaction (4) occurs readily in aqueous solutions of sodium borohydride, unless stabilised at high pH. The rate of this reaction varies with solution pH according to the following empirical equation established by Kreevoy and Jacobson [2],

$$\log t_{1/2} = \mathrm{pH} - (0.034T - 1.92) \quad (5)$$

where $t_{1/2}$ is the half-life in minutes for the decomposition of a $NaBH_4$ solution (i.e. the time taken for the $NaBH_4$ concentration to reduce to half), and T is the temperature in Kelvin. Accordingly, solutions are stabilised by the addition of alkali (usually NaOH). Alkali-stabilised borohydride solutions also hydrolyse in contact with many catalyst materials, limiting the number of suitable materials available for the anode electrocatalyst. Borate (BO_2^-) production resulting from borohydride oxidation (as well as from reaction (4)) could potentially be problematic since it has a low solubility and could limit the permitted level of discharge after which precipitation of borate might occur.

This paper presents preliminary data on cationic membranes for experimental DSBFCs. The cation exchange membrane route has been studied initially due to the ease of comparison with readily available commercial membranes such as Nafion. This program runs in parallel with the preparation of novel anion exchange membranes which will not be discussed in this paper.

2. Experimental

2.1. AC impedance

Twelve membranes were prepared by Cranfield University. In order to test the membranes easily they were divided into three batches. In order to fully hydrate the membrane samples, pieces approximately 3 cm × 3 cm were cut from the dry membrane sheet and placed in a glass sample tube and filled with deionised water (18 MΩ cm). The tubes were then heated to 95 °C in a water bath for 1 h. After cooling, the water in the sample tubes was replaced with 6 M NaOH, and the samples left overnight.

The Nafion® samples were prepared in a different manner to ensure that they were pure and fully hydrated. This was achieved by boiling in 3% hydrogen peroxide for 1 h, followed by rinsing in deionised water. They were then boiled in 0.5 M sulphuric acid for 1 h followed by boiling in deionised water for another hour and finally stored in deionised water until use. After conditioning the two Nafion samples were soaked in 6 M NaOH, this ensured that the sodium ion form of Nafion was obtained.

The samples were first tested in a 6 M NaOH solution using AC impedance. The AC impedance measurements were made using a computer controlled frequency response analyser (Solartron 1255B) and electrochemical interface (Solartron 1287) with Zplot and ZView software installed. Impedance experiments were conducted in the 0.1–100,000 Hz range with a 10 mV AC amplitude. Each experiment took about 9 min to complete.

The cell design is shown in Fig. 2. The glass cell is comprised of two identical halves, between which the membrane was held. Two Luggin capillaries were placed in close proximity to the membrane on either side. These held the saturated calomel (SCE) reference electrodes. Circular gold gauze electrodes (diameter 22 mm) were sited at each end of the cell. Solution was poured into the cell via the Luggin capillary ports before finally filling the Luggin capillaries and inserting the reference electrodes. The cell was water jacketed, which allowed water from the water bath to circulate and maintain the desired temperature. In the four electrode experiment, the connections from the Solartron 1287 were made as follows: the WE and CE were connected to each gold gauze electrode and the two reference electrodes connected to RE1 and RE2.

The membranes were subjected to a testing regime over 12 weeks. Membranes were tested in 6 M NaOH on day 0 and then in 25 wt% $NaBH_4$ in 6 M NaOH on days 1, 6, 9, 15, 29, 50 and 83. Membranes were tested in batches with the start date for each batch offset by 1 week.

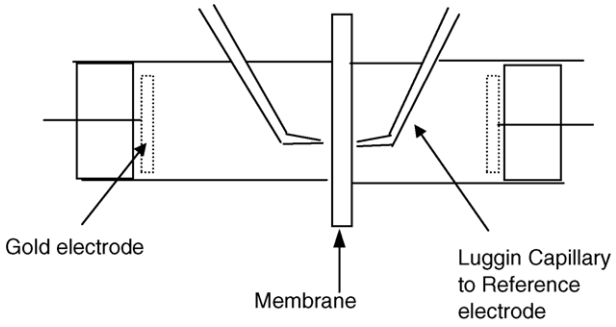

Fig. 2. Schematic of AC impedance cell.

2.2. Crossover studies

The method used to investigate the crossover of borohydride was as outlined by Mirkin and Bard [3]. The method links the maximum oxidation current of BH_4^-, under single sweep potentiodynamic conditions, to the concentration in the test solution, using a three-electrode cell comprising a gold working electrode, a chemically stable counter electrode and a saturated mercurous sulphate reference electrode (SMSE). The working electrode was a 0.2 mm diameter gold wire, sealed with epoxy resin into a glass capillary tube, the counter electrode was a 2 cm × 2 cm piece of nickel mesh, again sealed into a glass capillary, and the reference was a SMSE (Thermo-Electron Corp, Model SOOQ). The only deviation from the procedure described by Mirkin was the use of the nickel mesh counter electrode as opposed to RuO_2.

The electrodes were held together in a Perspex™ jig, which formed the top cover of a specially designed thermostatically-controlled two-compartment cell. The electrode assembly was connected to an EG&G Model 362 Scanning Potentiostat, the output from which was connected to an XY recorder.

The apparatus was calibrated in terms of the oxidation current versus the borohydride concentration by using accurately weighed solutions of 2, 4, 10, 50 and 100 mM sodium borohydride in 6 M NaOH. The solution compositions were verified by titration using the potassium iodate and sodium thiosulphate method of Lyttle et al. [4]. Calibration was performed at the beginning and end of each sample measurement.

The membrane samples were equilibrated in 6 M NaOH for a minimum of 16 h prior to being measured. The larger compartment of the cell was filled with 6 M NaOH, a magnetic stirrer bar added, and the cell lid containing the electrode assembly fitted. The smaller compartment was then filled with 30 wt% sodium borohydride in 6 M NaOH, the compartment lid fitted, and the test time started. The magnetic stirrer under the cell was set to stir slowly so as to prevent concentration polarisation, but not induce excessive turbulence.

Fig. 4. Equivalent circuit for the four electrode experimental set-up.

After a given time the stirrer was stopped and at least 60 s was allowed to lapse before the voltammetric sweep started. This allowed the liquid around the cell to become stationary; failure to do this resulted in spurious results.

The potentiostat was set to scan between −1300 and −300 mV (versus SMSE) at 100 mV s^{-1}, (displayed on the *X*-axis of the recorder) with the corresponding oxidation current displayed on the *Y*-axis. Measurement scans were normally taken at 1 h intervals and each scan was repeated after a short period (few seconds) of stirring followed by the 60 s equilibration time. The two values were then averaged.

2.3. Cell testing

A small compartment cell was used which compressed the membrane between the two halves. The membrane was held in place using a rubber flange with a 1 cm^2 hole cut into the middle. Each half comprised of a liquid reservoir with slots in the top in which the electrodes could be inserted.

The membrane was placed in between the two halves of the cell and then placed in a G-clamp to hold the cell together. Solution was then poured into both sides of the cell, 6 M NaOH on the cathode side and 25 wt% $NaBH_4$ in 6 M NaOH on the anode side. The cathode was a piece of carbon

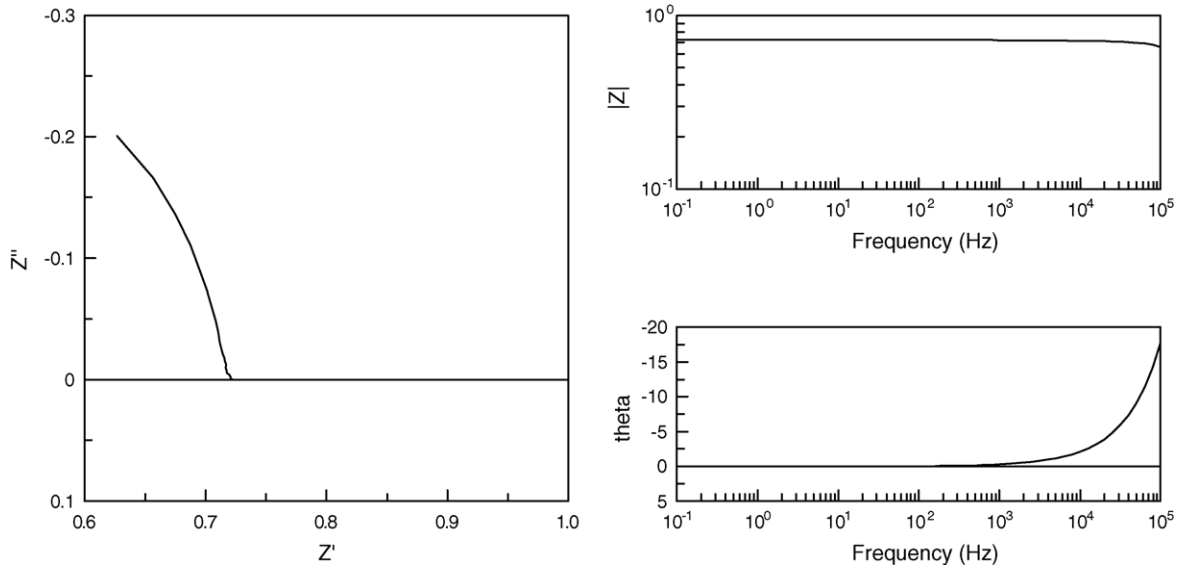

Fig. 3. Example complex (left) and Bode (right) plots from ZView.

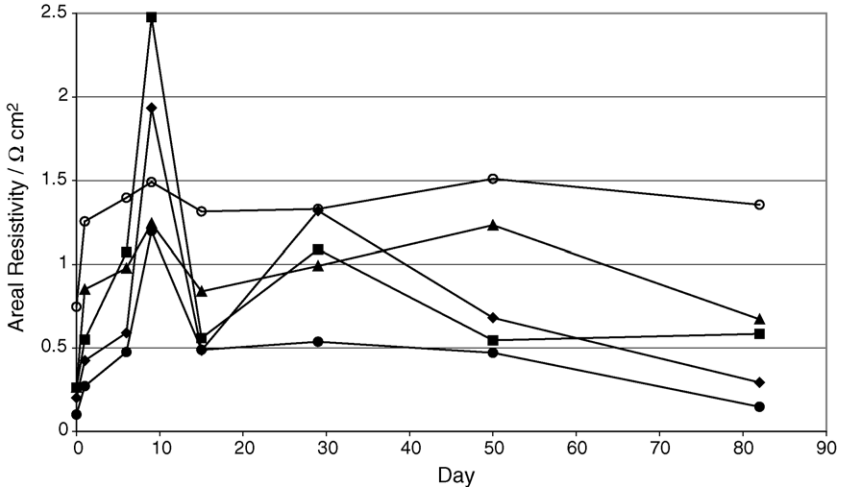

Fig. 5. Resistance of membranes against day of test for batch 1. (●): 3898P, (♦): 3541P, (■): 3542P, (▲): 3907P, (◯): empty cell.

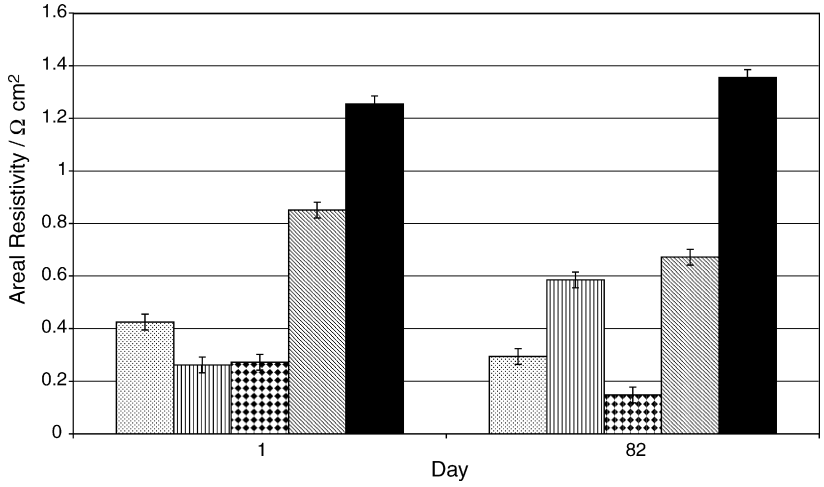

Fig. 6. Resistance against day for four membranes from batch 1. Dotted bar: 3541P, striped bar: 3542P, diamond filled bar: 3898P, diagonally striped bar: 3907P, filled bar: empty cell.

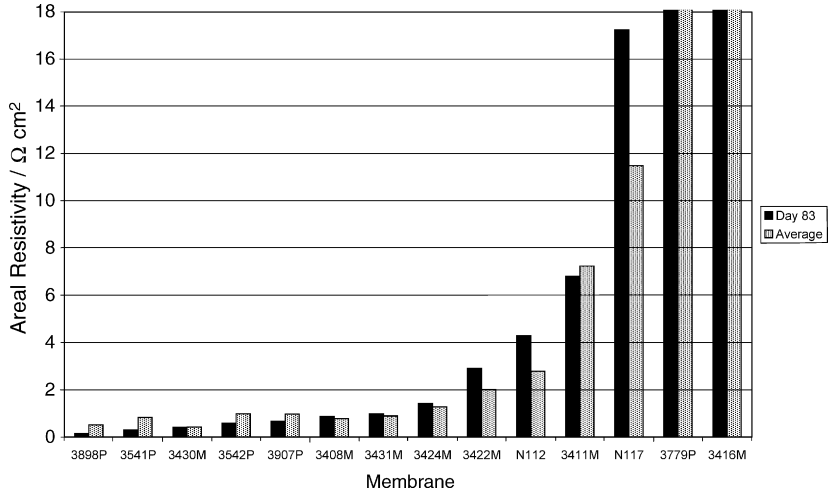

Fig. 7. Resistance at 83 days and the average resistance over 83 days for 14 membranes. Dark bar: Day 83, dotted bar: average.

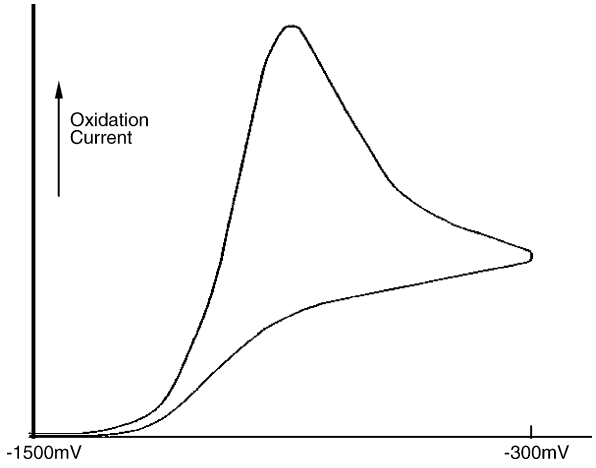

Fig. 8. Typical voltammogram of $NaBH_4$ in 6 M NaOH. Sweep rate 100 mV s^{-1}. Sweep from −1500 to −300 mV vs. SMSE.

paper coated in Pt/C (0.6 mg Pt cm^{-2}), and the anode was a 3 cm × 3 cm piece of gold gauze. The open circuit potential was allowed to settle before bubbling air into the cathode reservoir. The air was supplied from a compressed air line and passed through a bubbler containing soda lime to remove the carbon dioxide.

The polarisation curves were carried out using an electronic load (Kikusui PLZ334W). The current was increased steadily and the voltage recorded.

3. Results

3.1. AC impedance

Fig. 3 shows the typical plots obtained from ZView. The plots can be modelled using an equivalent circuit as shown in Fig. 4.

The resistance of the membranes was taken by the intercept of the vertical line of the complex plot with the *X*-axis. The membrane resistance, R_{mem} was normalised by using the following equation.

$$R_{men} = R_{tot} - R_{cell}$$

where R_{tot} is the sum of the membrane, R_{mem} and cell resistance, R_{cell}. R_{cell} was measured as the resistance of a cell filled with electrolyte but without a membrane.

Fig. 5 below shows the resistance of the membranes in batch 1 with time. The plot shows the four membranes in that batch along with the resistance of the cell without a membrane in order to see the slight fluctuations.

Though Fig. 5 shows the data obtained for batch 1, it is typical of the data obtained for all batches. In all cases the resistance increased on changing the test solution from 6 M NaOH to 25 wt% $NaBH_4$ in 6 M NaOH. However, after this, the resistance of the cell without a membrane present remained fairly constant at $1.3 \pm 0.1\ \Omega\ cm^{-2}$. The results from day 9 show a sharp increase in the resistance for the

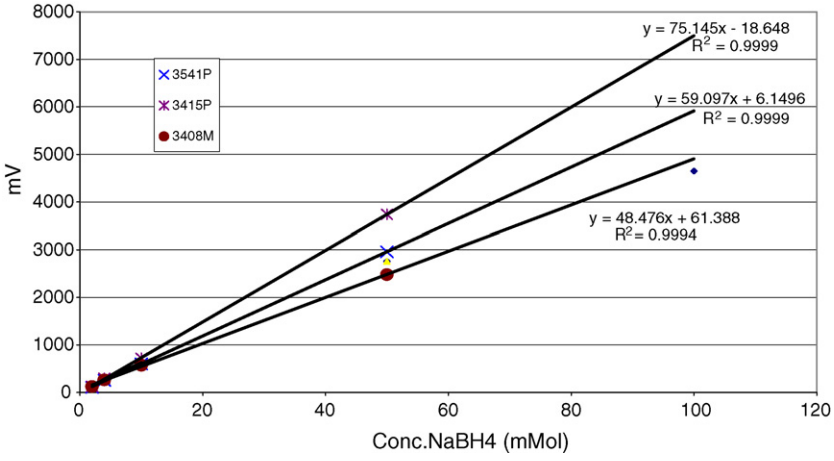

Fig. 9. Sodium borohydride concentration in 6 M NaOH vs. voltammeter reading for some typical membranes.

Table 3
Borohydride permeability data

Membrane	Areal resistivity ($\Omega\ cm^2$)	Thickness (μm)	Conductivity ($S\ cm^{-1}$)	Measured BH_4 crossover ($mol\ cm^{-2}\ s^{-1}$)	BH_4 Permeability ($mol\ cm^{-1}\ sec^{-1}$)	Conductivity/Permeability ($S\ mol^{-1}\ s$)
3408M	1.19	48	4.00E−03	2.07E−06	9.89E−09	4.0E05
3415M	0.44	213	4.80E−02	1.18E−06	2.54E−08	1.9E06
3541P	0.17	88	5.20E−02	4.59E−06	4.05E−08	1.2E06
Nafion 112	0.32	59	1.85E−02	3.59E−06	2.13E−08	8.9E05
Nafion 117	1.07	221	2.07E−02	4.01E−07	8.83E−09	2.3E06

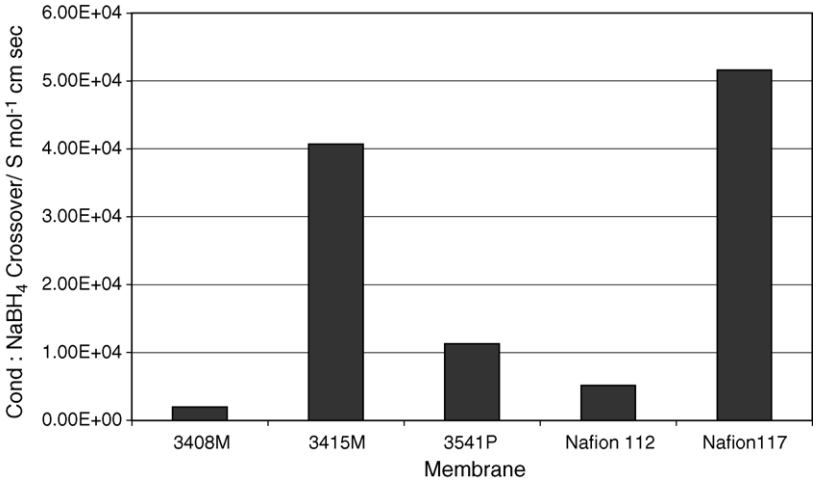

Fig. 10. Ratio of conductivity to borohydride crossover.

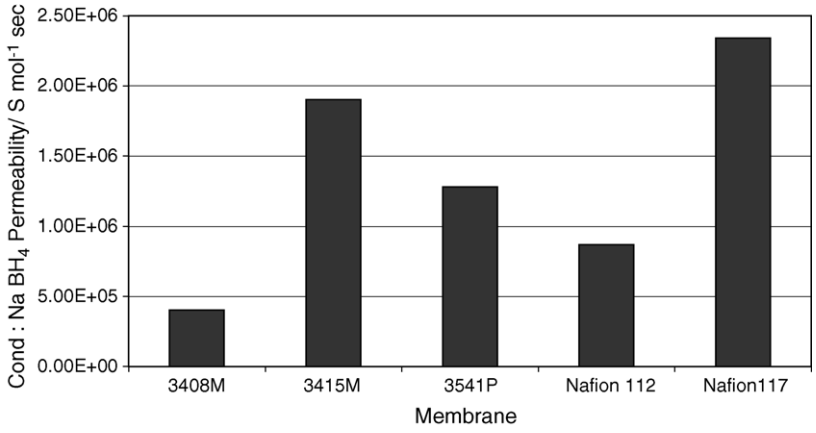

Fig. 11. Ratio of conductivity to borohydride permeability.

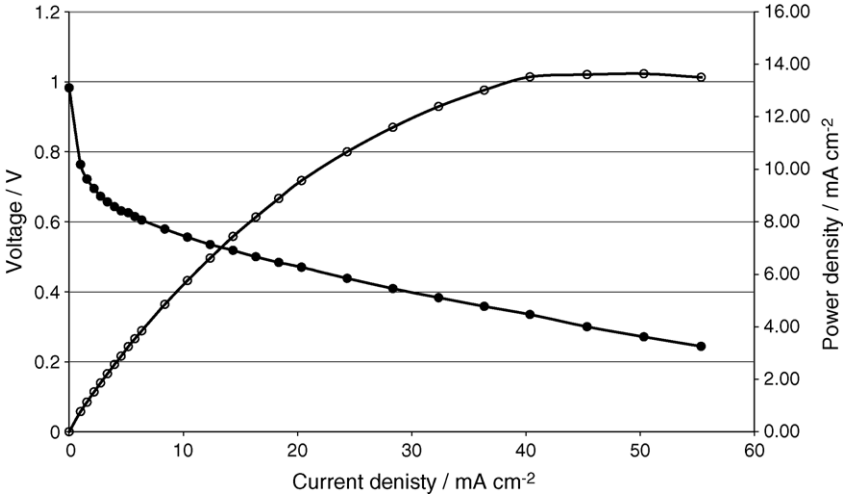

Fig. 12. Polarisation and power density curves for membrane 3898P in the compartment cell.

membrane samples in batch 1, however, this is only accompanied by a slight increase in the empty cell resistance, therefore not being directly related to the normalisation process. After day 15 the resistances become more consistent for the majority of the membranes, samples 3541P and 3542P show small increases again at day 29. Overall there is no significant change in the membrane resistance from day 1, when they were first exposed to the sodium borohydride solution and day 83 when they were finally tested. This is shown in Fig. 6, where the error bars shown represent the test to test error in the R_{cell} measurements.

Fig. 7 shows that for the majority of membranes there is no significant change between their average resistance and the resistance on day 83, indicating that, once in contact with 25 wt% sodium borohydride solution, there is little change in their properties. However, a small set of the membranes do show a difference, both Nafion samples show an increased resistance on the last day of testing compared to the average over the 83 days.

3.2. Borohydride migration

From the typical voltammogram shown in Fig. 8, the concentration of borohydride on the downstream side of the cell was calculated using the control measurements and plotted as a function of the diffusion time, as depicted in Fig. 9. This was repeated for each sample and the permeation rate was then derived from the slope of the line. The results for the membranes tested to date are given in Table 3.

Figs. 10 and 11 show the ratio of the membrane conductivity to borohydride crossover and permeability, respectively. The better membranes may be expected to have a high conductivity/crossover ratio, and this will be enhanced when the effect of membrane thickness is taken into account, as in Fig. 11.

3.3. Cell testing

Fig. 12 shows a sample polarisation curve obtained from the compartment cell. The plot shows that using this membrane sample in the compartment cell arrangement a maximum power density of 14 mA cm^{-2} can be achieved at 45 mA cm^{-2}.

4. Discussion and conclusions

A large number of membranes have been prepared by radiation grafting, the properties of which have been measured by AC impedance spectroscopy and electrochemical techniques.

The AC impedance spectroscopy compared 14 membranes including the commercially available Nafion 112 and Nafion 117. The results show that the resistance of many of the new membranes is lower than Nafion. The resistance of Nafion was found to increase towards the end of the 12-week test, which may be due borohydride solution causing degradation of the polymer membrane. The AC impedance testing involved the membrane samples being immersed in a 25 wt% $NaBH_4$ in 6 M NaOH solution for 12 weeks. None of the samples showed any physical deterioration whilst being stored in this harsh reducing environment, therefore showing that potentially these samples would stand up to long-term use in a fuel cell environment.

It can be seen from Table 2 that the borohydride migration (crossover), although very low, nonetheless varies over an order of magnitude in the membranes tested so far. Comparing the ratio of the crossover to the conductivity of the membrane, (Fig. 10), shows that, of those tested, Nafion 117 has the best 'figure of merit'. However, this membrane along with membrane 3415M, is also the thickest, and when the thickness is taken into account, as in Fig. 11, other membranes show similar performances. It may also be relevant to note that Nafion 112, although structurally identical to Nafion 117, has a lower figure of merit, perhaps indicating that the use of thicker membranes may be important in retarding the migration of the borohydride ion. Differences such as these have been seen previously between Nafion 117 and Nafion 112 in a proton environment [5].

The properties of the new membranes are borne out in Fig. 12 which shows a polarisation curve obtained using a small compartment cell with a Pt/C cathode and gold gauze anode. This compartment cell is not ideal in its design as a fuel cell but shows what can be readily achieved. Substitution of air with oxygen at the cathode should show significant improvements in performance and there is also the opportunity, owing to the alkaline environment, to employ a cheaper non-platinum catalyst at the cathode.

The results presented have shown that successful operation of a direct borohydride fuel cell can be obtained using a cation exchange membrane, in agreement with results obtained by Li et al. who used a Nafion 117 membrane [6]. However, to obtain the best performance from this form of cell it is believed an anion exchange membrane is needed, as this would negate the need for a sodium recirculation. There is also the potential to use hydrogen peroxide as the oxidant, which could give cell potentials of 3.02 V with the correct pH balance. With optimisation of the fuel cell design and components, the direct borohydride fuel cell will be a suitable power source for military application in an unmanned underwater vehicle.

References

[1] S.C. Amendola, P. Onnerud, M.T. Kelly, P.J. Petillo, S.L. Sharp-Goldman, M. Binder, J. Power Sources 84 (1999) 130.
[2] M. Kreevoy, R. Jacobson, Ventron Alembic 15 (1979) 2.
[3] M.V. Mirkin, A. Bard, J. Anal. Chem. 63 (1991) 532.
[4] D.A. Lyttle, E.H. Jensen, W.A. Struck, Anal. Chem. 24 (1952) 1843.
[5] S. Slade, S.A. Campbell, T.R. Ralph, F.C. Walsh, J. Electrochem. Soc. 149 (2002) A1556.
[6] Z.P. Li, B.H. Liu, K. Arai, K. Asaba, S. Suda, J. Power Sources 126 (2004) 28.